

Model averaging with mixed criteria for estimating high quantiles of extreme values: Application to heavy rainfall

Yonggwan Shin¹, Yire Shin^{2,*}, Jeong-Soo Park²

1: R&D Center, XRAI Inc., Gwangju 61186, Korea

2: Department of Statistics, Chonnam National University, Gwangju 61186, Korea

**: Corresponding author, e-mail: shinyire87@gmail.com*

June 13, 2025

Abstract

Accurately estimating high quantiles beyond the largest observed value is crucial in risk assessment and devising effective adaptation strategies to prevent a greater disaster. The generalized extreme value distribution is widely used for this purpose, with L-moment estimation (LME) and maximum likelihood estimation (MLE) being the primary methods. However, estimating high quantiles with a small sample size becomes challenging when the upper endpoint is unbounded, or equivalently, when there are larger uncertainties involved in extrapolation. This study introduces an improved approach using a model averaging (MA) technique. The proposed method combines MLE and LME to construct candidate submodels and assign weights effectively. The properties of the proposed approach are evaluated through Monte Carlo simulations and an application to maximum daily rainfall data in Korea. Additionally, theoretical considerations are provided, including asymptotic variance with random weights. A surrogate model of MA estimation is also developed and applied for further analysis.

Keywords: Bootstrap, generalized L-moment distance, profile likelihood, restricted maximum likelihood estimation, return level, surrogate model.

1 Introduction

The generalized extreme value (GEV) distribution (GEVD) is extensively used to model extremes in natural phenomena and human activities, such as hydrological events and incidents in insurance and financial markets (Coles 2001; Katz et al. 2002; Reiss & Thomas 2007). The primary reason for applying the GEVD is that it serves as a large-sample approximation to the

distribution of sample maximum, regardless of the population from which the data are drawn. The cumulative distribution function (CDF) of the GEVD is given by (Hosking & Wallis 1997):

$$F(x) = \exp \left\{ - \left(1 - \xi \frac{x - \mu}{\sigma} \right)^{1/\xi} \right\}. \quad (1)$$

when $1 - \xi(x - \mu)/\sigma > 0$ and $\sigma > 0$, where μ , σ , and ξ represent the location, scale, and shape parameters, respectively. The case where $\xi = 0$ in (1) corresponds to the Gumbel distribution. Notably, the sign of ξ in (1) differs from that used in Coles (2001) to align with the notation in Hosking & Wallis (1997). The tail behavior of the GEV distribution varies depending on the sign of ξ : it exhibits a heavy tail when $\xi < 0$, an exponential tail as $\xi \rightarrow 0$, and light or bounded when $\xi > 0$.

To estimate the three parameters of the GEVD, maximum likelihood estimation (MLE) and L-moment estimation (LME) methods are commonly used. The LME generally performs well with small samples and offers advantages over the MLE, including computational simplicity, greater robustness, and lower estimation variance (Hosking & Wallis 1997; Morrison & Smith 2002; Karvanen 2006; Delicado & Gorla 2008). Conversely, the MLE is preferable for large samples due to its desirable asymptotic properties.

Accurately estimating high upper quantiles is more critical than estimating the parameters of extreme value distributions, particularly in risk assessment and hydraulic structure design (Naghattini 2017; Allouche et al. 2023). For example, the 1% chance flood is computed at the 0.99 quantile of an extreme value distribution which is actually used by the US Federal Emergency Management Agency when developing its regulatory policy for floodplains (Grego & Yates 2024). When the upper endpoint is unbounded (or $\xi < 0$), estimating high quantiles of the GEVD with a small sample size becomes challenging because of larger uncertainties involved in model extrapolation. For instance, when $\xi = -0.35$ and the true 0.99 quantile is 443 (with $\mu = 100$ and $\sigma = 30$), the root mean squared errors (RMSEs) of the MLE and LME of 0.99 quantile with $n = 60$ are approximately 148 and 120, respectively. These RMSEs represent 33% and 27% of the true quantile, which is concerned as a substantial uncertainty.

In the context of the GEVD for block maxima data, several approaches have been proposed to address this issue, including a mixed estimation of the MLE and LME (Morrison & Smith 2002; Ailliot et al. 2011) and the application of a penalty function to the GEVD parameters (Coles & Dixon 1999; Bücher et al. 2021). The former method effectively and robustly estimates the parameters while reducing RMSE, whereas the latter can outperform MLE in certain situations depending on the choice of penalty function. Lekina et al. (2014) and Fabiola et al. (2021) introduced a semi-parametric and nonparametric weighted estimations of high quantiles, respectively, offering more flexibility and suitability than parametric methods. Daouia et al. (2024) presented general weighted pooled estimators of extreme quantiles calculated through a nonstandard geometric averaging scheme. These weighted estimation methods perform well for large sample sizes. Karvanen (2006) considered an estimation of quantile mixtures via L-moments and

trimmed L-moments. Grego et al. (2015) used finite mixture models to accommodate annual peak streamflow. Evin et al. (2011) and Totaro et al. (2024) explored using two-component mixtures of Gumbel distributions. Our study builds upon this framework by introducing a modified approach that employs mixtures of narrow extreme value submodels.

In this study, we propose a new estimation method to improve the accuracy of high quantile estimation in the GEVD using model averaging (MA). The MA combines the strengths of multiple candidate models by assigning greater weights to superior models (Liu et al. 2016; Fletcher 2018). Unlike traditional model selection, which discards all but the best model, MA explicitly accounts for model uncertainty by integrating information from competing statistical models. MA reduces the risk of model misspecification and makes predictions less sensitive to model assumptions. By incorporating model uncertainty, MA produces more accurate estimates and reliable confidence intervals than model selection from frequentist and Bayesian perspectives (Burkland et al. 1999; Hoeting et al. 1999; Claeskens & Hjort 2008). Le and Clarke (2022) showed that MA is asymptotically better than model selection for prediction.

However, the MA method has some limitations, such as computational cost. The slowest candidate model indicates the overall computational speed of MA. Additionally, MA does not consistently outperform model selection. Model selection is preferred when the error variance is small and identifying the best model is relatively straightforward. Conversely, MA performs well when the error variance is large (Liu et al. 2016, 2023). Given the high error variance in estimating high quantiles of the GEVD under a negative shape parameter, MA may outperform some existing methods.

Several Bayesian MA approaches for extreme values have been developed based on the likelihood function and posterior probability (Raftery et al. 2005; Sabourin et al. 2013; Vettori et al. 2020). These approaches typically estimate the parameters of candidate models using MLE or Bayes estimators and assign weights based on marginal likelihood. In frequentist MA, candidate model parameters are estimated using the least squares method or MLE, and weights are determined based on information criteria, cross-validation, or an unbiased risk estimator (Claeskens & Hjort 2008; Wang et al. 2009).

This study applies different criteria for estimation and weighting in MA, primarily utilizing L-moments. This mixed application of criteria is a key aspect of the proposed method, which was motivated by Morrison & Smith (2002) and Ailliot et al. (2011). We hypothesize that the mixed-criteria approach—where candidate model parameters are estimated using MLE and weights are assigned based on L-moments, or vice versa—may outperform the conventional single-criterion method, which estimates parameters via MLE and assigns weights based on the likelihood function. We anticipate that this mixed-criteria approach will improve the estimation of high quantiles of extreme values. To our knowledge, L-moment-based MA methods have been scarcely studied, despite the popularity of non-MA approaches based on L-moments in climatology and hydrology (Hosking & Wallis 1997; Naghettini 2007; Kjeldsen et al. 2017; Hong et al. 2022; Strong et al. 2025, for example among many). We consider two methods: (1)

estimating candidate model parameters using MLE and calculating weights using the generalized L-moments distance, and (2) estimating candidate model parameters using LME and calculating weights using the smooth Akaike information criterion. For comparison, we also evaluate other methods, including mixed estimation (Morrison & Smith 2002; Ailliot et al. 2011) and a penalized likelihood method (Coles & Dixon 1999).

The rest of this paper is structured as follows: Section 2 details the proposed MA methods. Theoretical considerations on the MA estimator and uncertainty calculation under random weights are presented in Section 3. Section 4 provides a simulation study. Section 5 presents an application using maximum rainfall data from Hae-nam, Korea. Discussion and conclusion are provided in Sections 6 and 7. Supplementary Material includes additional details such as formulas, tables, and figures. The R code for our implementation is available on GitHub: <https://github.com/yire-shin/MA-gev.git>.

2 Model averaging methods

The MA methodology consists of three steps: (1) constructing candidate models, (2) estimating model parameters, and (3) calculating weights for each candidate model (Liu et al. 2023; Salaki et al. 2024; Hao et al. 2024). The primary objective of MA in this study is to improve the estimation of high quantiles of extreme values rather than to focus on estimating the parameters of the GEVD. The $1/p$ return level, denoted as $r_{1/p}$, represents the $1 - p$ quantile of the distribution (Coles 2001). The “T-year return level” is commonly used for annual extreme values, where $T = 1/p$. The MLE and LME of the three GEVD parameters are defined as follows:

$$\hat{\theta}_M = (\hat{\mu}_M, \hat{\sigma}_M, \hat{\xi}_M), \quad \hat{\theta}_L = (\hat{\mu}_L, \hat{\sigma}_L, \hat{\xi}_L). \quad (2)$$

2.1 Construction of candidate models

A concrete application of MA often requires an initial selection of several candidate models. These candidate models may differ entirely or only in certain components. Among three parameters in GEVD, estimating the shape parameter ξ is more challenging than others. Additionally, ξ is dimensionless, and the behavior of GEVD is more sensitive to ξ than the other two parameters. Therefore, the proposed method starts with the shape parameter ξ . We consider two approaches for initializing our MA algorithm: the MLE of ξ and the LME of ξ .

In the first approach, based on $\hat{\xi}_M$, we construct a $100 \times (1 - \alpha)$ confidence interval for ξ using the profile likelihood (Coles 2001). For instance, setting $\alpha = 0.05$ provides a 95% confidence interval (C_L, C_U) . We select K values of ξ proportionally distributed according to the profile likelihood of ξ within this interval from C_L to C_U , since values near the lower and upper bounds are less probable than those in the interior. In the second approach, based on $\hat{\xi}_L$, we use a nonparametric bootstrap to construct a $100 \times (1 - \alpha)$ confidence interval for ξ . Subsequently, we select K values of ξ proportionally (with equal probability) from the bootstrap distribution

of $\hat{\xi}_L$ within this confidence interval. This study considers two values of α : 0.05 and 0.10. The upper panel of Figure 1 illustrates how the proposed method selects ten values of ξ_k s using a 95% confidence interval of ξ based on the profile likelihood function.

For each selected ξ_k , we estimate μ_k and σ_k using either the MLE or LME, keeping ξ_k fixed. These estimators are denoted as $\hat{\mu}_{kM}$, $\hat{\sigma}_{kM}$, and $\hat{\mu}_{kL}$, $\hat{\sigma}_{kL}$, respectively. Estimating two other parameters with ξ_k fixed is computationally simpler and yields lower standard errors (SE) than estimating all three GEVD parameters. When ξ is known, the LMEs of μ_k and σ_k are given by:

$$\begin{aligned}\hat{\sigma}_k &= \frac{l_2 \xi_k}{(1 - 2^{\xi_k}) \Gamma(1 + \xi_k)}, \\ \hat{\mu}_k &= l_1 - \hat{\sigma}_k \{1 - \Gamma(1 + \xi_k)\} / \xi_k,\end{aligned}\tag{3}$$

where l_1 and l_2 are the first and second sample L-moments computed from the data. As a result, we obtained K GEV candidate models, where each is the two-parameter GEVD. From each candidate model, we compute the T-year return level ($\hat{r}_{T,k}$) using the estimated parameters ($\hat{\mu}_{kM}$, $\hat{\sigma}_{kM}$, ξ_k) or ($\hat{\mu}_{kL}$, $\hat{\sigma}_{kL}$, ξ_k). Finally, we compute the MA T-year return levels by averaging these T-year return levels with weights w_k , which are nonnegative and summed to one.

2.2 Weighting scheme based on L-moments distance

When the parameters in each candidate model are estimated using the MLE, reusing the likelihood value to compute weights—such as through the smooth Akaike information criterion (AIC) (Claeskens & Hjort 2008; Fletcher 2018)—may not necessarily improve estimation, in our view. As demonstrated later in this study, conventional model averaging that employs MLE for parameter estimation and smooth AIC for weight assignment does not perform well, at least in our simulation study. Therefore, we explored alternative criteria to construct more informative weights.

For a three-parameter distribution, the L-moment distance for each candidate model M_k is defined as follows, subject to the constraint that $\xi > -1$ for the GEVD:

$$LD_k = |l_1 - \lambda_{1,k}| + |l_2 - \lambda_{2,k}| + |l_3 - \lambda_{3,k}|,\tag{4}$$

where l_j represents the j th sample L-moment, and λ_j denotes the j th population L-moment, for $j = 1, 2, 3$. The sample L-moments are computed directly from the data, whereas $\lambda_{j,k}$ values are derived from the GEVD using the estimated parameters for each candidate model M_k . L-moments offer both theoretical and practical advantages over conventional moments. Specifically, they exhibit lower sensitivity to outliers and provide more reliable identification of the parent distribution generating the data (Hosking & Wallis 1997; Lomba & Alves 2020).

Since the LME is obtained by solving equations that ensure (4) equals zero, we aim to assign higher weights to submodels with smaller L-moment distances. This weighting scheme is preferable because L-moments characterize the distribution differently from the likelihood function.

One challenge in using the L-moment distance is that the three L-moments operate on different scales. Typically, the first term in (4) dominates the distance metric, while the third term—corresponding to the crucial shape parameter—is nearly negligible. To address this issue, we introduce a generalized L-moment distance (GLD) for each model M_k :

$$\text{GLD}_k = d_k^T V_k^{-1} d_k, \quad (5)$$

where $d_k^T = (l_1 - \lambda_{1,k}, l_2 - \lambda_{2,k}, l_3 - \lambda_{3,k})$, and V_k is a 3×3 covariance matrix of d_k . A similar GLD approach has been explored in previous studies, including Kjeldsen & Prosdocimi (2015) for regional frequency analysis as well as Alvarez et al. (2022).

To compute V_k for each model, one can use a parametric bootstrap based on the GEVD with parameter estimates $(\hat{\mu}_{kM}, \hat{\sigma}_{kM}, \xi_k)$ since an explicit form of V_k is unavailable. However, this approach is computationally intensive. To mitigate this issue, we approximated V_k using the covariance matrix of the sample L-moments (Elamir & Seheult 2004), treating $\lambda_{j,k}$ as constants. For this computation, we employed the ‘lmomco’ package (Asquith 2014) in R. However, in some cases, this method resulted in a non-positive definite covariance matrix. In such instances, we computed the covariance matrix using a nonparametric bootstrap. Once computed, V was fixed and applied uniformly across all K candidate models, as it no longer depended on k .

To assign higher weights to submodels with smaller GLD_k values, we adopted the multivariate normal probability:

$$p(\underline{x}|M_k) = \frac{1}{(2\pi)^{3/2} |V|^{1/2}} \exp(-d_k^T V^{-1} d_k / 2). \quad (6)$$

The weight for model M_k is calculated as follows:

$$\hat{w}_k = \frac{p(\underline{x}|M_k)}{\sum_{k=1}^K p(\underline{x}|M_k)}, \quad (7)$$

which ensures that $\sum_{k=1}^K w_k = 1$ and that all w_k values remain within the range $[0, 1]$. This weight can be interpreted as the probability that model M_k is the best among the set of candidate models. Given that sample L-moments generally converge to a multivariate normal distribution as $n \rightarrow \infty$ (Hosking 1990), the function in (6) serves as an approximation of the likelihood function of population L-moments given three sample L-moments.

For a more robust L-moment distance, one can replace l_1 and l_2 with the median and interquartile range of the data. While l_2 is proportional to Gini’s mean difference and thus already serves as a robust scale estimate, l_1 (the sample mean) is not (Ailliot et al. 2011). To address this, we substitute the first element of d_k with the median distance (sample median $- q_{0.5}$) as an alternative to (5). In the following sections, we refer to this alternative weighting scheme as the ‘med’ weight.

The lower panel of Figure 1 illustrates how the proposed method computes the return level estimate using a weighted average of return values from 10 submodels. The 200-year return level obtained via the MA method lies between the estimates derived from the MLE and LME.

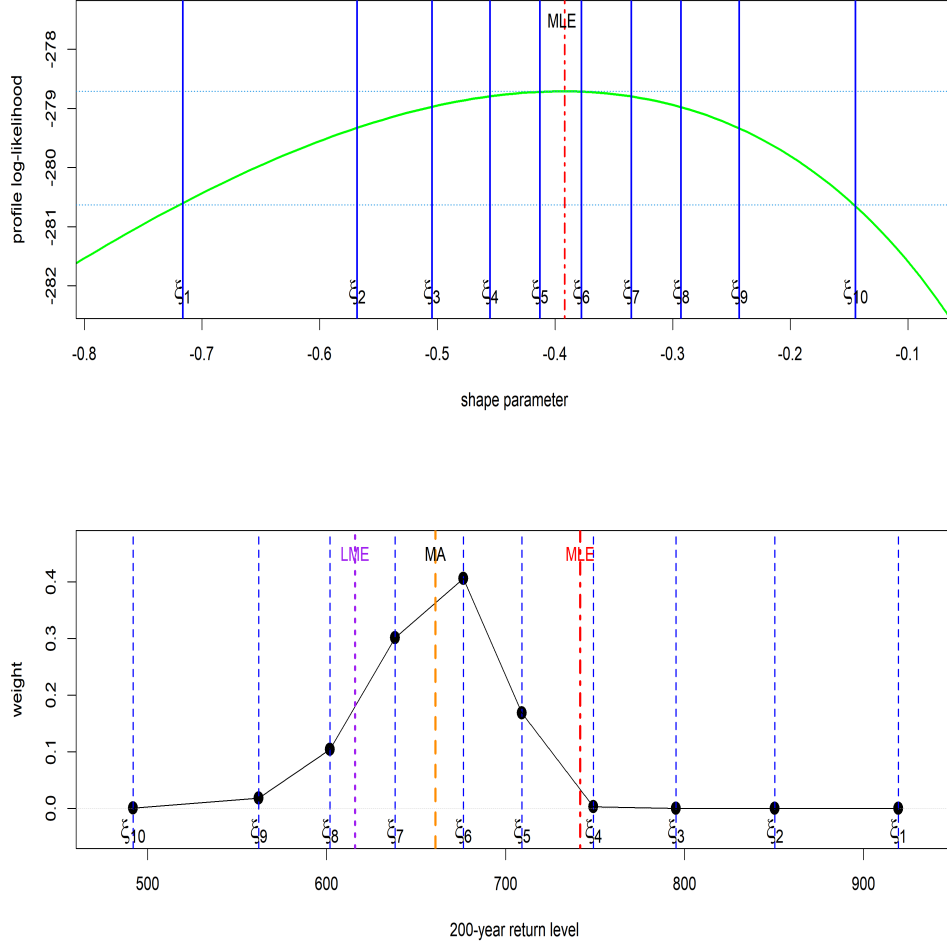


Figure 1: Illustration of the selection of ξ_k s values using the profile likelihood of ξ and the corresponding weights, based on annual maximum daily rainfall data (unit: mm) from Hae-nam, Korea. (Top panel): The green curve represents the profile log-likelihood function, while the 10 vertical lines indicate the selected ξ_k s values. (Bottom panel): The 200-year return level estimates from 10 submodels (vertical dotted lines) are shown along with their corresponding weights (black dots) for the proposed MA method (‘like1’). The return level estimates obtained from the MLE, LME, and MA methods are also displayed for comparison.

2.3 Estimation of high quantiles and building a surrogate model

Our MA method estimates the high quantile or T-year return level using the following formulation:

$$\hat{r}_{\text{MA}} = \sum_{k=1}^K \hat{w}_k \hat{r}_k, \quad (8)$$

which is a weighted average of the return level predictions from individual submodels. We aim to achieve this with lower uncertainty than the MLE, LME, and other established methods.

The limitation of this MA approach is that it may not be useful for system description and understanding (Fletcher 2018). We consider constructing a weighted averaged (or ensemble) model from the K GEV candidate models to address this limitation. However, the ensemble model may not necessarily follow a GEVD, even though each model M_k does. Thus, simply taking a weighted sum of K GEV candidate models is not an ideal solution. Instead, we propose building a surrogate model that still follows a GEVD and best approximates the return level estimates generated by the MA method.

To achieve this, we estimate the three GEVD parameters by minimizing the following function with respect to μ , σ , and ξ :

$$RSS(\mu, \sigma, \xi) = \sum_{i=1}^I (r_{q_i} - \hat{r}_{q_i})^2, \quad (9)$$

where $\{r_{q_i}\}_{i=1,\dots,I}$ are the return levels, corresponding to probability q_i , computed from a $GEVD(\mu, \sigma, \xi)$, and \hat{r}_{q_i} are the corresponding return level estimates obtained using the MA method. To ensure a broad coverage of important quantiles, we selected 16 probabilities ranging from 0.5 to 0.999. Although the surrogate model is only an approximation and may not be theoretically exact, it is computationally convenient and useful for further data analysis. This convenience includes additional predictions, model comparison, and model diagnostics such as quantile-per-quantile and return level plots. Of course, other models could also be used as surrogates instead of reusing the GEVD.

3 Theoretical consideration

3.1 Conditional expectation

We provide a theoretical justification for why the proposed MA method is expected to perform well. If we assume that $r(\hat{\mu}, \hat{\sigma}, \hat{\xi})$ is an unbiased estimator of the return level $r(\mu, \sigma, \xi)$, then we have:

$$r(\mu, \sigma, \xi) = E\{r(\hat{\mu}, \hat{\sigma}, \hat{\xi})\} = E_{\xi} \left[E\{r(\hat{\mu}, \hat{\sigma}, \hat{\xi}) \mid \hat{\xi} = \xi\} \right]. \quad (10)$$

If $E\{r(\hat{\mu}, \hat{\sigma}, \hat{\xi}) \mid \hat{\xi} = \xi\}$ serves as an estimator of $r(\mu, \sigma, \xi)$, then it is unbiased and has a smaller variance than $r(\hat{\mu}, \hat{\sigma}, \hat{\xi})$, as follows from the conditional variance identity (Casella & Berger 2001),

$$\begin{aligned} Var\{r(\hat{\mu}, \hat{\sigma}, \hat{\xi})\} &= Var \left[E\{r(\hat{\mu}, \hat{\sigma}, \hat{\xi}) \mid \hat{\xi} = \xi\} \right] + E \left[Var\{r(\hat{\mu}, \hat{\sigma}, \hat{\xi}) \mid \hat{\xi} = \xi\} \right] \\ &\geq Var \left[E\{r(\hat{\mu}, \hat{\sigma}, \hat{\xi}) \mid \hat{\xi} = \xi\} \right]. \end{aligned} \quad (11)$$

If $\hat{\xi}$ is a sufficient statistic for $r(\mu, \sigma, \xi)$, then $E\{r(\hat{\mu}, \hat{\sigma}, \hat{\xi}) \mid \hat{\xi} = \xi\}$ is a uniformly better-unbiased estimator, as stated by the Rao-Blackwell theorem (Casella & Berger 2001). However,

$E\{r(\hat{\mu}, \hat{\sigma}, \hat{\xi}) \mid \hat{\xi} = \xi\}$ is not an estimator, as it depends on the unknown parameter ξ . To address this, we approximate $E\{r(\hat{\mu}, \hat{\sigma}, \hat{\xi}) \mid \hat{\xi} = \xi\}$ using a weighted average of available estimators computed for values of ξ s near $\hat{\xi}$, leveraging relatively simple estimation methods.

Since estimating ξ is more challenging than estimating the other parameters of the GEVD and because $\hat{\xi}$ has the most substantial influence on the estimation of $r(\mu, \sigma, \xi)$ —particularly when $\xi < -0.2$ —conditioning ξ as a fixed value near $\hat{\xi}$ can substantially simplify the estimation process. The generally lower variability of a narrow submodel compared to a broader model is well demonstrated in Claeskens & Hjort (2008) under the local misspecification framework. Additionally, fitting submodels is computationally more efficient than fitting a full model.

Assuming that $(\hat{\mu}, \hat{\sigma}, \hat{\xi})$ can always be estimated from the data, a heuristic derivation of \hat{r}_{MA} proceeds as follows:

$$\begin{aligned}
E \left[r\{\hat{\mu}, \hat{\sigma}, \hat{\xi}\} \mid \hat{\xi} = \xi \right] &= E \left[r\{\hat{\mu}_2(\xi), \hat{\sigma}_2(\xi), \xi\} \mid \hat{\xi} = \xi \right] \\
&\quad \left(\begin{array}{l} \hat{\mu}_2(\xi), \hat{\sigma}_2(\xi) \text{ are 2-dimensional} \\ \text{estimators for a given constant } \xi \end{array} \right) \\
&= \int r\{\hat{\mu}_2(\xi), \hat{\sigma}_2(\xi), \xi\} \times p \left[r\{\hat{\mu}_2(\xi), \hat{\sigma}_2(\xi), \xi\} \mid \hat{\xi} = \xi \right] dr \\
&\quad \left(\begin{array}{l} \hat{\mu}_2(\xi), \hat{\sigma}_2(\xi) \text{ are no more random} \\ \text{for a given constant } \xi \text{ and the data} \end{array} \right) \quad (12) \\
&= r\{\hat{\mu}_2(\xi), \hat{\sigma}_2(\xi), \xi\} \\
&\quad \xleftarrow{\text{estimate}} \sum_{k=1}^K r\{\hat{\mu}_2(\xi_k), \hat{\sigma}_2(\xi_k), \xi_k\} \times \hat{w}(\xi_k),
\end{aligned}$$

where ξ_k values are selected based on the sampling distribution of ξ . Thus, our MA method can be interpreted as integrating out the ξ parameter.

3.2 Asymptotic distribution of MA return level

When submodel M_k is fitted using the MLE, the MLE of (μ_k, σ_k) for a given ξ_k follows asymptotically a normal distribution with mean (μ_k, σ_k) and covariance matrix Σ_k , which is the inverse of the Fisher information matrix, provided that $-1 < \xi_k < 1/2$ (Bücher et al. 2021, for example). Consequently, \hat{r}_k asymptotically follows a normal distribution with mean r_k and variance:

$$\text{Var}(\hat{r}_k) \approx \nabla r_k^T \Sigma_k \nabla r_k, \quad (13)$$

by the delta method, where ∇r_k is a gradient vector of r_k with respect to (μ_k, σ_k) . For the GEV distribution, the gradient vector of r_k with respect to (μ_k, σ_k) is given by: $\nabla r_k = [1, \xi_k^{-1}(1 - y_p^{\xi_k})]^T$, for given ξ_k , where $y_p = -\ln(1 - p)$.

We assume that the true return level is composed of a model average of the return levels

$(r_{k,true})$ from the submodels :

$$r_{true} = \sum_{k=1}^K w_k r_{k,true}. \quad (14)$$

Let $\hat{w}_n(k)$ and $\hat{r}_n(k)$ represent the weight and return level estimates obtained from data with sample size n . Additionally, let v_k denote the asymptotic variance of \hat{r}_k , as provided in (13). Define W_k as a random variable such that $\hat{w}_n(k) \xrightarrow{D} W_k$ as $n \rightarrow \infty$, where $E(W_k) = w_k$. Then we have the following result for asymptotic distribution of MA return level estimator:

Theorem 1: When submodel M_k is fitted using the MLE, we have, as $n \rightarrow \infty$

$$\sum_{k=1}^K \hat{w}_n(k) \hat{r}_n(k) - r_{true} \xrightarrow{D} \Lambda_{MA} = \sum_{k=1}^K w_k \Lambda_k \quad (15)$$

where $\Lambda_k \sim AN(0, v_k)$.

Proof: Let R_k be a normal random variable such that $\hat{r}_n(k) \xrightarrow{D} R_k \sim AN(r_{k,true}, v_k)$. Then, we have:

$$\begin{aligned} \sum_{k=1}^K \hat{w}_n(k) \hat{r}_n(k) - r_{true} &= \sum_{k=1}^K \{\hat{w}_n(k) - W_k\} \hat{r}_n(k) + \sum_{k=1}^K W_k \hat{r}_n(k) - r_{true} \\ &= \sum_{k=1}^K \{\hat{w}_n(k) - w_k\} \hat{r}_n(k) + \sum_{k=1}^K (w_k - W_k) \hat{r}_n(k) + \sum_{k=1}^K W_k \hat{r}_n(k) - r_{true} \end{aligned} \quad (16)$$

Since $\hat{w}_n(k)$ is uniformly integrable, it follows that $E[\hat{w}_n(k)] \rightarrow w_k$, which implies that $\hat{w}_n(k) \xrightarrow{P} w_k$ (Serfling 1980). Thus, the above equation simplifies to:

$$\begin{aligned} &\xrightarrow{D} \sum_{k=1}^K (w_k - W_k) R_k + \sum_{k=1}^K W_k R_k - \sum_{k=1}^K w_k r_{k,true} \\ &= \sum_{k=1}^K w_k (R_k - r_{k,true}) = \sum_{k=1}^K w_k \Lambda_k. \end{aligned} \quad (17)$$

The Slutsky theorem and continuity theorem of weak convergence are applied in the above derivation. This establishes the statement of the theorem. \square

Unlike the individual Λ_k , the limiting random variable Λ_{MA} is no longer normally distributed. The mean and variance of Λ_{MA} are given as $E(\Lambda_{MA}) = 0$ and

$$Var(\Lambda_{MA}) = \underline{w}^T C \underline{w}, \quad (18)$$

where $\underline{w}^T = (w_1, \dots, w_K)$ and C is $Var(\underline{\Lambda})$ which is the asymptotic covariance matrix of $\hat{\underline{r}}$, where $\underline{\Lambda}^T = (\Lambda_1, \dots, \Lambda_K)$.

When submodel M_k is fitted using the LME, the mixed method of Morrison & Smith (2002) and Ailliot et al. (2011) or the penalized likelihood method of Coles & Dixon (1999), the estimators also follow an asymptotic normal distribution with the corresponding covariance matrix. Therefore, Theorem 1 remains valid for these estimators as well.

3.3 Asymptotic variance of MA return level

The diagonal elements of C , the asymptotic variances of \hat{r} , are obtained using (13). However, the off-diagonal elements of C , representing the covariances $\text{Cov}(\hat{r}_i, \hat{r}_j)$ for $i \neq j$, are difficult to compute explicitly. To address this, we considered a variance formula directly from (8):

$$\text{Var}(\hat{r}_{\text{MA}}) = \sum_{k=1}^K w_k^2 \text{Var}(\hat{r}_k) + \sum_{i \neq j}^K w_i w_j \text{Cov}(\hat{r}_i, \hat{r}_j). \quad (19)$$

If the correlation coefficient (ρ_{ij}) between r_i and r_j is known, the second term on the right-hand side can be computed using the following formula:

$$\text{Cov}(\hat{r}_i, \hat{r}_j) = \rho_{ij} \sqrt{\text{Var}(\hat{r}_i)} \sqrt{\text{Var}(\hat{r}_j)}. \quad (20)$$

To approximate ρ_{ij} , we use the Pearson correlation coefficient between models M_i and M_j , based on estimated values from both models. These estimated values include, for example, selected quantiles and parameter estimates. Specifically, we use nine quantile estimates ranging from 0.1 to 0.9 in increments of 0.1, along with the three-parameter estimates ($\hat{\mu}_i$, $\hat{\sigma}_i$, and ξ_i). These 12 values are treated as 12 observations for approximating the correlation.

3.4 MA variance with random weights

For computing $\text{Var}(\Lambda_{\text{MA}})$ in real applications with data of size n , we may need to replace \underline{w} in (18) with its estimate $\hat{\underline{w}}^T = (\hat{w}_1, \dots, \hat{w}_K)$. In this case, $\hat{\underline{w}}$ is a random vector derived from the sample, meaning that the formula (18) may need to be adjusted to account for the uncertainty in $\hat{\underline{w}}$. To calculate $\text{Var}(\Lambda_{\text{MA}})$ using the random vector $\hat{\underline{w}}$, we assume that $\hat{\underline{w}}$ and $\hat{\underline{r}}$ are independent. The expression for the variance is then given by:

$$\begin{aligned} \text{Var}(\hat{r}_{\text{MA}}) &= \text{Var}(\hat{\underline{w}}^T \hat{\underline{r}}), \text{ where } \hat{\underline{r}}^T = (\hat{r}_1, \dots, \hat{r}_K) \\ &= \text{Var}_{\hat{\underline{w}}} [E(\hat{\underline{w}}^T \hat{\underline{r}} | \hat{\underline{w}})] + E_{\hat{\underline{w}}} [\text{Var}(\hat{\underline{w}}^T \hat{\underline{r}} | \hat{\underline{w}})] \\ &= \text{Var}_{\hat{\underline{w}}} [\hat{\underline{w}}^T E(\hat{\underline{r}})] + E_{\hat{\underline{w}}} [\hat{\underline{w}}^T C \hat{\underline{w}}] \\ &= E(\hat{\underline{r}})^T D E(\hat{\underline{r}}) + \text{tr}(D C) + E(\hat{\underline{w}})^T C E(\hat{\underline{w}}), \end{aligned} \quad (21)$$

where $D = \text{Var}(\hat{\underline{w}})$. In the last equation, we used the formula $E(\hat{\underline{w}}^T C \hat{\underline{w}}) = \text{tr}(D C) + E(\hat{\underline{w}})^T C E(\hat{\underline{w}})$ (Ravishanker et al. 2022, for example). Here, C is approximated by the asymptotic covariance matrix (\hat{C}), computed using (13) and (20), and evaluated at $\hat{\underline{r}}$. Due to the additional uncertainty introduced by the randomness of the weights, this variance must be greater than or equal to the asymptotic variance in (19) for fixed weights.

We need to estimate $E(\hat{\underline{w}})$, $E(\hat{\underline{r}})$, and D from the data for practical purposes. However, deriving these theoretically from (7) is challenging. One possible approach is to use bootstrapping to approximate these quantities, although we did not adopt this method in our study. Instead, we assume a distribution for $\hat{\underline{w}}$. Given that $0 \leq \hat{w}_k \leq 1$ for $k = 1, \dots, K$ and that weights $\sum_{k=1}^K \hat{w}_k = 1$, it is reasonable to assume that $\hat{\underline{w}}$ follows a Dirichlet distribution with parameter vector \underline{w} , where $0 \leq w_k \leq 1$ for $k = 1, \dots, K$ and $\sum_{k=1}^K w_k = 1$. Then, under this assumption,

$$E(\hat{w}_k) = w_k, \quad \text{Var}(\hat{w}_k) = w_k(1 - w_k)/2, \quad \text{Cov}(\hat{w}_i, \hat{w}_j) = -w_i w_j/2 \quad (22)$$

for all $i \neq j$. These quantities form the elements of D . The covariance matrix D can then be approximated by substituting $\hat{\underline{w}}$ in place of \underline{w} , yielding the estimated matrix by \hat{D} .

To approximate $E(\hat{\underline{r}})$, we used a moving average of order q for $\hat{\underline{r}}$ instead of directly substituting $\hat{\underline{r}}$ into $E(\hat{\underline{r}})$. With these approximations, we obtain $\text{Var}(\hat{r}_{\text{MA}})$ in (21) using the following formulation:

$$\widehat{\text{Var}}(\hat{\underline{w}}^T \hat{\underline{r}}) \approx \widehat{\underline{r}}(q)^T \hat{D} \widehat{\underline{r}}(q) + \text{tr}(\hat{D} \hat{C}) + \hat{\underline{w}}^T \hat{C} \hat{\underline{w}}. \quad (23)$$

where $\widehat{\underline{r}}(q)^T$ is the order q moving average of $\hat{\underline{r}}^T = (\hat{r}_1, \dots, \hat{r}_K)$. We chose $q = 3$ in this study.

This formula is computationally much faster than using bootstrap to estimate $E(\hat{\underline{w}})$, $E(\hat{\underline{r}})$, and D . This expression for the MA variance with random weights has not been previously documented in the literature.

4 Simulation study

4.1 Computing strategy

Selecting the number (K) of candidate models is necessary in the proposed method. One recommended strategy is to start with a relatively large K (e.g., $K = 15$) and then remove submodels with small weights, such as those with $w_k \leq 0.01$. Additionally, if the weight assigned to the smallest ξ_k or the largest ξ_k remains above a certain threshold (e.g., 0.2), the method adds a few additional x_{i_k} values beyond the lower or upper bounds. The weights are then recalculated using the updated number of submodels, K' , and the MA return level estimate \hat{r}_{MA} is obtained using the new weight vector $\hat{\underline{w}}'^T = (\hat{w}'_{i_1}, \dots, \hat{w}'_{i_{K'}})$.

Thus, selecting between 90% and 95% confidence intervals for choosing ξ_k s values may no longer be critically important, as we adjust ξ_k s flexibly based on the assigned weights. For the same reason, selecting the initial method—whether using the profile likelihood in the MLE or bootstrap samples in the LME—to select ξ_k is also not crucial. A pilot simulation study in the Supplementary Material indicates that variations in the starting method ('mle' or 'lme') do not produce substantially different results. Similarly, selecting different confidence levels (90% or 95%) does not lead to substantial performance disparities. Therefore, in this study, we use the 95% confidence interval based on the profile likelihood ('mle' starter) of ξ to select ξ_k .

Additionally, we considered a ‘conventional’ model averaging approach in which the parameters of each GEV_k submodel are estimated using the MLE, and submodels are weighted based on smooth AIC scores. Here, the smooth AIC score (Claeskens & Hjort 2008) is defined as $\Delta AIC_k = AIC_k - \min_K AIC_k$, so that the weight is obtained by:

$$\hat{w}_k = \frac{\exp(-\Delta AIC_k/2)}{\sum_{k=1}^K \exp(-\Delta AIC_k/2)}. \quad (24)$$

For comparative purposes, we consider two existing modified MLE methods. The mixed method proposed by Morrison & Smith (2002) and Ailliot et al. (2011) has at least two versions: (1) Re.MLE1 – This approach estimates the parameters by maximizing the likelihood under the constraint that the population mean (λ_1) is equal to the sample mean (l_1), and (2) Re.MLE2 – This version is obtained by maximizing the likelihood under the additional restrictions that

$$\lambda_1 = l_1, \quad \lambda_2 = l_2, \quad (25)$$

where λ_2 and l_2 represent the second population and sample L-moments, respectively.

The penalized likelihood method proposed by Coles and Dixon (1999) estimates the parameters by maximizing the following penalized log-likelihood:

$$l_{pen}(\mu, \sigma, \xi) = \ln(L(\mu, \sigma, \xi)) + \ln(p(\xi)), \quad (26)$$

where $L(\mu, \sigma, \xi)$ is the likelihood function and $p(\xi)$ is a penalty function applied to ξ :

$$p(\xi) = \begin{cases} 1 & \text{if } \xi \geq 0 \\ \exp\{-\lambda(\frac{1}{1+\xi} - 1)^\alpha\} & \text{if } -1 < \xi < 0 \\ 0 & \text{if } \xi \leq -1 \end{cases} \quad (27)$$

with the hyperparameters $\alpha = 1$ and $\lambda = 1$. We refer to the estimator obtained using this method as ‘MLE.CD,’ where CD stands for Coles and Dixon (1999).

For the LME, we utilized the ‘Lmoments’ or ‘lmomco’ packages in R, as provided by Karvanen (2006), based on the methods of Hosking (1990) and Asquith (2014). For the MLE, return level plots, and confidence interval based on profile likelihood, we primarily used the ‘ismev’ package (Coles 2001) in R. Additionally, for constrained optimization under (25), we employed the ‘Rsolnp’ package.

As presented in the Supplementary Material, a pilot simulation study revealed that MA methods exhibited substantial underestimation of return levels when $\xi \leq -0.3$. We applied a trimming approach to address this issue, removing the smallest observations. The abbreviations of the MA and other methods used in this study are listed in Table 1, where ‘trim=1’ and ‘trim=2’ indicate the cases where the minimum and second minimum observations, respectively, were excluded during estimation or weighting. Additionally, based on another pilot simulation study, we found that the weighting schemes ‘gLd’ and ‘med’ did not result in substantial performance differences. Therefore, for simplicity—given that 12 methods are already considered—the MA method with ‘med’ weighting is omitted from this simulation study.

Table 1: Abbreviations of the model averaging and other methods used in this study. Here, ‘gLd’ represents the generalized L-moments distance defined in (5), the weighting formula using smooth AIC is provided in (24), the constraints for Re.MLE is defined in (25), and the penalty function for MLE.CD is given in (27).

method name	estimation	weighting
MA.gLd1	MLE	gLd/trim=1
MA.gLd2	MLE	gLd/trim=2
MA.like0	LME	smooth AIC/trim=0
MA.like1	LME	smooth AIC/trim=1
MA.cvt	MLE	smooth AIC
Re.MLE1	MLE/constraint-1	
Re.MLE2	MLE/constraint-2	
MLE.CD	MLE/penalty-CD	

4.2 Simulation setting

To evaluate the performance of the MA methodology, we conducted a simulation study in which high quantiles were known by generating random numbers from a GEVD. This study estimates the 100-year and 200-year return levels (corresponding to the 0.99 and 0.995 quantiles) using a sample size of $n = 50$. The number of submodels (K) was set to 12, and the number of bootstrap samples was 500. We generated 1,000 random samples to compute the following evaluation measures for comparing different estimators:

$$\text{Bias} = \bar{\hat{r}} - r, \quad \text{SE} = \left\{ \frac{1}{N} \sum_{i=1}^N (\hat{r}_i - \bar{\hat{r}})^2 \right\}^{1/2}, \quad \text{RMSE} = \left\{ \frac{1}{N} \sum_{i=1}^N (\hat{r}_i - r)^2 \right\}^{1/2}, \quad (28)$$

where r denotes the true return level, $\bar{\hat{r}} = \sum_{i=1}^N \hat{r}_i / N$, \hat{r}_i is the return level estimate from the i th sample, and N represents the number of simulation samples ($N = 1,000$). Lower values of SE and RMSE are preferable.

The upper endpoint of the GEVD is bounded when $\xi > 0$ (in Hosking-Wallis notation). As a result, estimating high quantiles of the GEVD when $\xi > 0$ is relatively straightforward, and the RMSE values tend to be smaller. The MLE and LME typically perform well when $\xi \geq 0$. Therefore, we focus on cases when ξ ranges in $(-0.5, 0.0)$. The case $\xi \leq -0.5$ is not considered because the GEVD has no finite variance in this range. We conduct experiments for 10 values of ξ : $\xi = -0.45, -0.4, -0.35, -0.3, -0.25, -0.2, -0.15, -0.1, -0.05, -0.001$. For better interpretability, we set $\mu = 100$ and $\sigma = 30$, as estimates of these parameters are equivariant (Casella & Berger 2001). Setting $\mu = 0$ and $\sigma = 1$ often results in values less than one with decimal points, making distinguishing differences among methods in the summary table harder. Additionally, this (0,1) scaling occasionally produces negative values, which in rare cases can

cause numerical issues in computing the likelihood function or inverting the Hessian matrix.

4.3 Simulation results

Table 2 and Figure 2 present the simulation results for bias, SE, and RMSE computed for the quantile $q_{0.99}$ using 10 estimation methods. Acronyms for the method names are provided in Table 1. Since the results for the ‘gLd’ and ‘med’ weighting schemes were similar in this simulation study, only the results for the ‘gLd’ weight are included in Table 2.

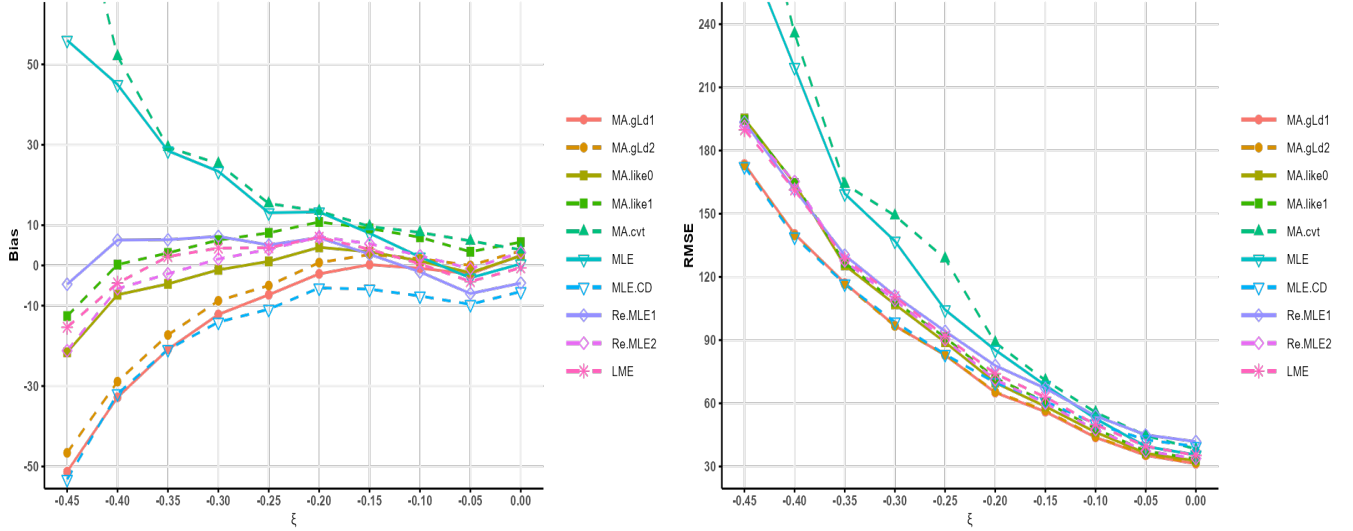


Figure 2: Same as Table 2 but for the bias (left) and RMSE (right).

Regarding bias, the MLE exhibits overestimation (positive bias), particularly when $\xi \leq -0.15$, while the proposed MA methods with ‘gLd’ weight and MLE.CD display underestimation (negative bias), especially for $\xi \leq -0.3$. The LME, Re.MLEs, and MA.likes generally perform well. For cases where $-0.25 < \xi < 0$ (moderately heavy-tailed distributions), the LME, MA.gLds, and MA.like0 perform well, producing small biases. For $-0.35 \leq \xi \leq -0.25$, MA.like0, Re.MLE2, and LME show good performance. For extremely heavy-tailed case ($\xi < -0.35$), Re.MLE1 and MA.like1 perform well in terms of bias.

Regarding SE and RMSE, for $\xi \leq -0.25$, MA.gLds and MLE.CD exhibits smaller SE values, resulting in lower RMSE than other methods. However, this reduction in SEs is primarily due to severe underestimation, making the lower RMSE in these cases less meaningful. Nevertheless, it is noteworthy that MA.gLds remains both the smallest SE and bias for $-0.25 < \xi \leq 0$, leading to genuinely lower and meaningful RMSEs. For $-0.35 \leq \xi \leq -0.25$, MA.likes, Re.MLE2, and LME yield smaller RMSE values than other methods. Determining the best-performing methods for $\xi < -0.35$ is difficult, but LME, Re.MLEs, and MA.likes are acceptable choices.

Based on these findings, the most suitable method depends on the value of ξ : MA.gLds for

Table 2: Simulation results of the bias, standard error (SE), and root mean squared error (RMSE) of the GEVD, computed for the quantile $q_{0.99}$, using the 10 estimation methods across 10 values of ξ . The sample size is $n = 50$, with parameters $\mu = 100$ and $\sigma = 30$. Acronyms of the method names are provided in Table 1.

Measure	Method	-.45	-.4	-.35	-.3	-.25	-.2	-.15	-.1	-.05	0
Bias	MA.gLd1	-51.3	-32.8	-20.9	-12.2	-7.3	-2.1	0.2	-0.7	-2.1	2.5
Bias	MA.gLd2	-46.6	-28.9	-17.3	-8.8	-5.0	0.7	2.7	1.7	0.0	3.6
Bias	MA.like0	-21.6	-7.3	-4.6	-1.1	1.0	4.5	3.4	1.1	-1.8	2.4
Bias	MA.like1	-12.6	0.2	3.1	6.3	8.1	10.8	9.2	7.0	3.4	5.8
Bias	MA.cvt	104.2	52.0	29.4	25.3	15.4	13.5	9.7	8.2	6.1	3.9
Bias	MLE	56.0	45.0	28.5	23.4	13.1	13.3	8.0	2.1	-3.1	0.4
Bias	MLE.CD	-53.2	-31.9	-20.9	-14.1	-10.9	-5.6	-5.9	-7.6	-9.7	-6.5
Bias	Re.MLE1	-4.7	6.3	6.4	7.2	5.1	6.9	2.8	-1.6	-7.0	-4.4
Bias	Re.MLE2	-21.2	-5.8	-2.1	1.6	4.0	7.1	5.4	2.4	-0.8	3.2
Bias	LME	-15.4	-4.4	2.2	4.3	4.4	7.0	4.0	0.4	-4.0	-0.6
SE	MA.gLd1	165.8	136.5	115.2	96.0	82.6	65.1	56.0	43.8	35.2	31.2
SE	MA.gLd2	166.5	136.7	115.3	96.3	82.8	65.4	56.5	44.1	35.5	31.5
SE	MA.like0	194.0	164.1	125.4	107.0	89.0	69.7	58.4	46.3	36.3	32.6
SE	MA.like1	194.2	164.6	126.7	108.1	90.9	71.2	60.0	47.4	37.1	33.1
SE	MA.cvt	316.7	229.7	161.4	146.9	127.8	87.8	70.2	55.1	44.3	38.1
SE	MLE	273.1	214.8	156.9	135.0	103.6	84.3	68.0	52.7	39.4	35.5
SE	MLE.CD	164.0	135.3	114.8	97.6	82.5	69.6	60.6	49.6	41.6	39.0
SE	Re.MLE1	193.4	161.4	130.1	112.9	94.1	77.6	67.0	54.0	44.5	41.6
SE	Re.MLE2	190.3	165.1	127.6	108.9	90.1	70.8	59.8	47.4	37.3	33.6
SE	LME	189.3	161.2	128.7	110.5	91.7	73.7	62.8	49.9	39.4	35.3
RMSE	MA.gLd1	173.6	140.4	117.1	96.8	82.9	65.1	56.0	43.8	35.3	31.3
RMSE	MA.gLd2	172.9	139.7	116.6	96.7	83.0	65.4	56.6	44.1	35.5	31.7
RMSE	MA.like0	195.2	164.3	125.5	107.0	89.0	69.8	58.5	46.3	36.3	32.7
RMSE	MA.like1	194.6	164.6	126.7	108.3	91.3	72.0	60.7	47.9	37.3	33.6
RMSE	MA.cvt	333.4	235.5	164.1	149.1	128.7	88.8	70.9	55.7	44.7	38.3
RMSE	MLE	278.8	219.5	159.5	137.0	104.4	85.3	68.5	52.7	39.5	35.5
RMSE	MLE.CD	172.4	139.0	116.7	98.6	83.2	69.8	60.9	50.2	42.7	39.5
RMSE	Re.MLE1	193.5	161.5	130.3	111.1	94.2	77.9	67.1	54.0	45.0	41.8
RMSE	Re.MLE2	191.5	165.2	127.6	108.9	90.2	71.2	60.0	47.5	37.3	33.8
RMSE	LME	189.9	161.3	128.7	110.6	91.8	74.0	62.9	49.9	39.6	35.3

$-0.25 < \xi \leq 0$, MA.likes, Re.MLE2, and LME for $-0.35 \leq \xi \leq -0.25$, and MA.like1, Re.MLE1, and LME for $\xi < -0.35$. Considering bias and RMSE, MLE and MA.cvt do not perform well for the range over $\xi < 0$. Without specifying the ξ value, Re.MLEs, LME, and MA.likes are generally reliable methods.

5 Real data application

For a real-data example, we analyzed a time series of annual maximum daily precipitation (unit: *mm*) recorded in Hae-nam, Korea. The dataset consists of 52 observations from 1971 to 2022 and is available at <https://github.com/yire-shin/MA-gev/tree/main/data>. We selected this weather station because the data exhibits a heavy right tail, making it well-suited for evaluating the effectiveness of the proposed methods. Figure 3 displays the relative frequency histogram with density curves and a scatterplot with lines representing the 50-year return level estimates.

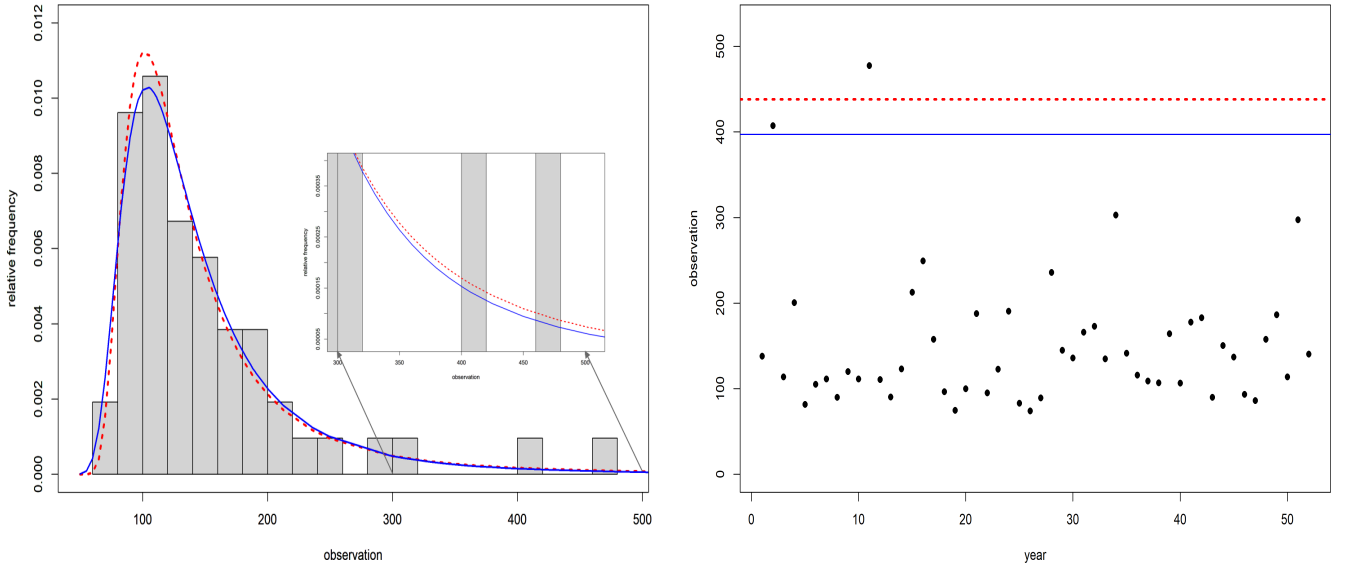


Figure 3: (Left) Density plots overlaid on the relative frequency histogram and (Right) a scatterplot of observations by year with horizontal lines representing the 50-year return level estimates. The data depicts the annual maximum daily rainfall (unit: *mm*) in Hae-nam, Korea. Both figures' blue solid line and red dashed line correspond to the estimates obtained using the LME and MLE methods.

Table 3 presents the parameter estimates, 100-year return levels, and their SE obtained using the formula (21) and nonparametric bootstrap (NpB) with 500 resamples for 10 estimation methods. Parameter estimates for the MA methods are derived from the surrogate models. In Table 3, the asymptotic SEs of MA.gLds (MA.likes) obtained using the formula (21) are greater

(less) than the corresponding SEs computed via nonparametric bootstrap. The SE (NpB) of MA methods is smaller than other methods, whereas MLE, MLE.CD, and Re.MLE1 yield larger SEs. The SEs of Re.MLE2 and LME fall within the moderate range—the 100-year return levels estimated by MA.likes and Re.MLE2 lies between those obtained using LME and MLE. Based on the findings from the simulation study, the return levels of MA.gLds may be underestimated despite their small SE (NpB) values. Conversely, the return level estimated by MLE may be overestimated, with exceptionally large SEs in both asymptotic and bootstrap calculations.

Table 3: Estimates of parameters ($\hat{\mu}$, $\hat{\sigma}$, $\hat{\xi}$), 100-year return level (100-y RL), and their asymptotic standard errors (Asym. SE) computed using the formula (21) and nonparametric bootstrap (NpB) for 10 estimation methods applied to the annual maximum rainfall data (unit: *mm*) in Hae-nam station, Korea.

Method	$\hat{\mu}$	$\hat{\sigma}$	$\hat{\xi}$	100-y RL	Asym. SE	SE (NpB)
MA.gLd1	115.3	34.34	-0.336	492.2	73.0	66.3
MA.gLd2	115.1	34.35	-0.342	498.5	74.1	67.6
MA.like0	113.4	34.72	-0.351	511.5	67.3	92.3
MA.like1	114.8	33.94	-0.363	518.1	72.1	93.9
MLE	112.6	35.10	-0.394	569.4	204.8	211.8
MLE.CD	113.3	35.23	-0.348	513.5		130.2
Re.MLE1	111.5	33.88	-0.382	537.1		133.2
Re.MLE2	112.8	34.58	-0.356	515.7		103.8
LME	113.5	37.35	-0.310	494.9		96.1

Figure 4 presents the sampling distributions of 100-year return levels from nine estimation methods, displayed as density plots over the relative frequency histogram, based on 1,000 bootstrap samples. Except for MLE, all distributions appear approximately normal, though some exhibit slight right skewness.

Figure 5 presents quantile-per-quantile plots for nine estimation methods. We used the standard plotting position formula: $q_i = (i - 0.5)/n$ to construct these plots. Surrogate models were utilized for the MA methods. The plots for MLE and Re.MLE1 appear to overestimate the largest observation, whereas the other methods fit the data relatively well.

Figure 6 presents the return level plots for nine estimation methods. This figure was generated using the ‘gev.rl’ function from the ‘isnev’ package in R. To compute the covariance matrix of parameter estimates required for ‘gev.rl’, we employed a nonparametric bootstrap with 500 repetitions. Because of the simplicity of interpretation, and because the choice of scale compresses the tail of the distribution so that the effect of extrapolation is highlighted, return level plots are particularly convenient for both model presentation and validation (Coles 2001). In Figure 6, the MA methods exhibit the narrowest confidence bands, while Re.MLE2 and LME

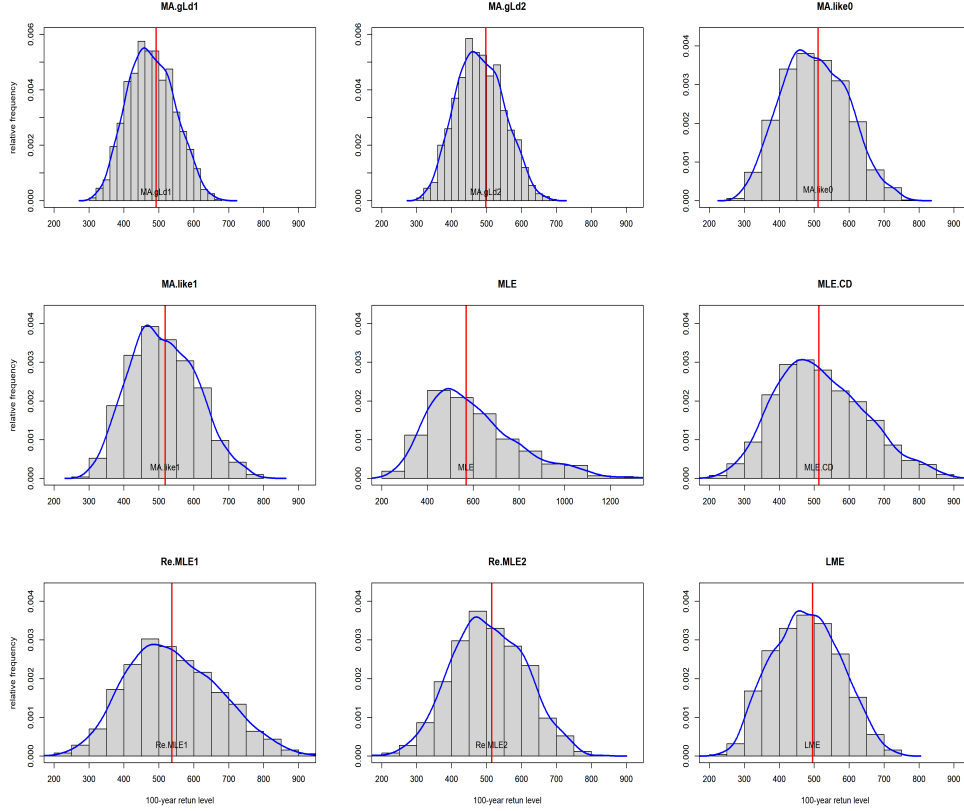


Figure 4: Sampling distributions of 100-year return levels from nine estimation methods, displayed as density plots over the relative frequency histogram. These distributions were obtained using 1,000 bootstrap samples from the annual maximum daily rainfall data (unit: *mm*) in Hae-nam, Korea. Acronyms for the method names are provided in Table 1.

show the second-best performance among the nine methods.

6 Discussion

6.1 Bias correction and Bayesian model averaging

The proposed MA methods with ‘gLd’ and ‘med’ weights exhibit negative biases despite the left-trimming approach adopted in this study, mainly when ξ is less than -0.3 . To address this issue, a bias correction technique may be necessary. Bayesian model averaging (BMA) could provide a solution for correcting such biases. BMA assigns weights proportional to the model’s marginal likelihood (Hoeting et al. 1999; Raftery et al. 2005; Shin et al. 2019; Vettori et al. 2020, for example among many). The BMA framework begins by specifying prior probabilities $p(M_k)$ for all candidate models M_1, \dots, M_K and defining the prior density $p(\underline{x}|M_k)$. The distribution

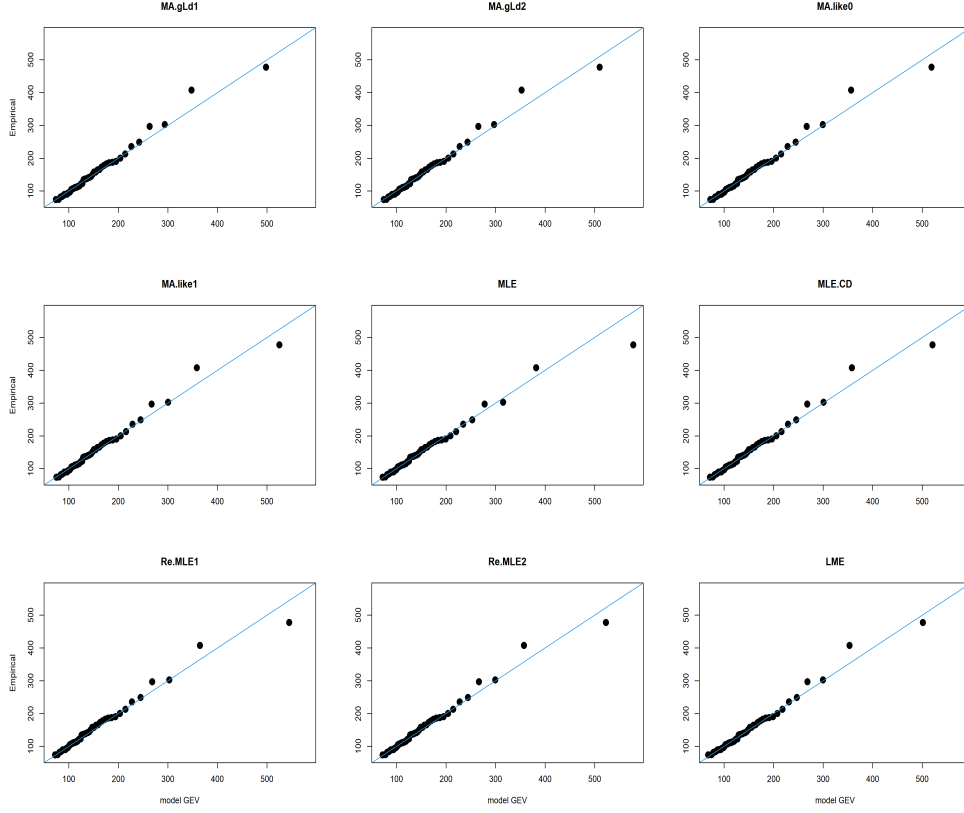


Figure 5: Quantile-per-quantile plots of nine methods fitted to the annual maximum daily rainfall (unit: *mm*) data in Hae-nam, Korea.

of the return level given the data (\underline{x}) is then expressed as:

$$p(r|\underline{x}) = \int p(r, M_k|\underline{x}) dM_k \approx \sum_{k=1}^K p(r|M_k, \underline{x}) p(M_k|\underline{x}). \quad (29)$$

Here, $p(M_k|\underline{x})$ can be expressed using Bayes' theorem as follows:

$$p(M_k|\underline{x}) = \frac{p(\underline{x}|M_k) p(M_k)}{\sum_{k=1}^K p(\underline{x}|M_k) p(M_k)}, \quad (30)$$

where $p(\underline{x}|M_k)$ is typically the likelihood of model M_k and $p(M_k)$ represents the prior probability of M_k . The posterior mean and variance of the BMA-predicted return level are given by (Hoeting et al. 1999; Claeskens & Hjort 2008)

$$\begin{aligned} E(r|\underline{x}) &= \sum_{k=1}^K E(r|M_k, \underline{x}) w_k, \\ Var(r|\underline{x}) &= \sum_{k=1}^K [E(r|M_k, \underline{x}) - E(r|\underline{x})]^2 w_k + \sum_{k=1}^K Var(r|\underline{x}, M_k) w_k, \end{aligned} \quad (31)$$

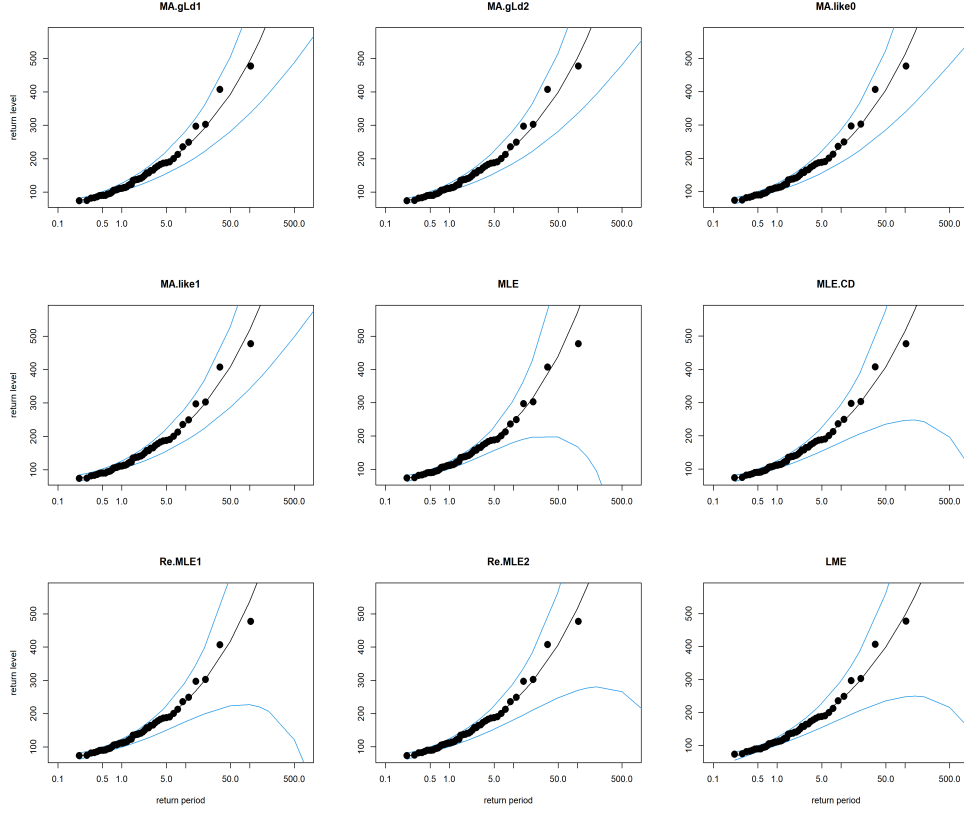


Figure 6: Return level plots for nine estimation methods applied to the annual maximum daily rainfall data (unit: *mm*) from Hae-nam, Korea.

where weight w_k is the same to (30). For estimating return level in the GEV, we estimate $E(r|M_k, \underline{x})$ by $r(\hat{\mu}_2(\xi_k), \hat{\sigma}_2(\xi_k), \xi_k)$ in this study. Then the estimator of $E(r|\underline{x})$ in (31) is the same as \hat{r}_{MA} in (8), but with different weights. The weights in (7) and (24) do not use the prior $p(M_k)$, which is different from the weights in (31).

For the prior of M_k , we consider the prior for the shape parameter ξ only, which is similar to a reversed form of the penalty function of Coles and Dixon (1999):

$$p(M_k) = p(\xi_k) = \begin{cases} 1 & \text{if } \xi_k \leq -1 \text{ or } \xi_k \geq 0 \\ 1 - 2\xi_k & \text{if } -1.0 < \xi_k < 0. \end{cases} \quad (32)$$

We employed this function mainly for bias correction of \hat{r}_{MA} because our estimator \hat{r}_{MA} with ‘gLd’ weighting scheme turned out to underestimate the true return level for negative ξ (especially for $\xi \leq -0.3$) in the simulation study. By providing more weight for ξ_k closer to -1.0 , we expected the return level estimator to correct the underestimation bias of \hat{r}_{MA} .

The results of a simulation study using BMA with the above prior (32) showed only a little (about 5-7%) reduction of biases for $\xi \leq -0.3$ and the new addition of overestimation biases for $\xi > -0.3$. In other words, we did not successfully correct the underestimation bias of \hat{r}_{MA} using

the above BMA scheme, so we do not document the results in this report. However, we believe that a more elaborate application of BMA than that employed in this study can find an answer to improve the estimation of high quantiles with accuracy.

6.2 Weighting scheme based on forward cross-validation

Contrary to the L-moments distance approach, many researchers have used cross-validation (CV) to determine weights for MA. Hansen and Racine (2012) proposed jackknife MA, where weights are selected based on leave-one-out CV. For time series MA, forward CV has been considered to preserve the temporal order in prediction (Hjorth 1982; Zhang & Zhang 2023). Although the data in this study are assumed to be stationary, we applied the forward CV approach to the weights selection, as our primary goal is to predict high quantiles, mainly out-of-sample quantities (i.e., extrapolative predictions).

To determine weights based on forward CV, we first rearrange the data in ascending order. We then hold out the largest $\alpha\%$ of values as a test set and use the remaining $(100 - \alpha)\%$ of the data—referred to as the training set—to estimate the parameters of each submodel. For each submodel, we predict the test set value using the submodel trained on the training set and compute the forward CV (FCV) score as follows:

$$FCV_k = \sum_{i=1}^{n_{te}} \frac{\{y_i^{te} - \hat{y}_{i,k}^{te}\}^2}{s_{i,k}^2}, \quad (33)$$

where the superscript ‘te’ denotes the test set, n_{te} is the number of observations in the test set, and $s_{i,k}^2 = \text{Var}(\hat{y}_{i,k}^{te})$ represents the variance estimate of the prediction, obtained in Section 3.4. Here, $\hat{y}_{i,k}^{te}$ is computed using the plotting position estimation, where the parameters are estimated from the training set. To compute $\hat{y}_{i,k}^{te}$, we consider the MLE and LME within each submodel M_k . A smaller value of FCV_k indicates better extrapolative prediction performance, which is desirable when working with a limited number of extreme observations. To assign a higher weight to submodels with smaller FCV_k values, we adopted the following likelihood function of the normal distribution:

$$p(\underline{x}|M_k) = \prod_{i=1}^{n_{te}} \frac{1}{\sqrt{2\pi} s_{i,k}} \times \exp\left(-\frac{FCV_k}{2}\right). \quad (34)$$

Then, the weight for model M_k is calculated using the same formula as in (7). In addition to assigning weights using (34), we also attempted to determine weights by minimizing (33) through a numerical optimization routine. Zhang and Zhang (2023) established the asymptotic optimality of weights that minimize $\sum_{i=1}^{n_{te}} \left(y_i^{te} - \hat{y}_{i,k}^{te}\right)^2$ for time series data.

However, throughout our simulation study and real-data applications, we observed that the performance of the MA method with weights based on FCV is susceptible to the proportion of the training set (also referred to as the window size). We found that an appropriate proportion for reliable estimation depends on the return period and tail heaviness. In this study, we could

not systematically determine an optimal proportion that simultaneously accounts for both the return period and tail heaviness. Nevertheless, we believe that the FCV is a promising criterion for weight assignment and should be further investigated in future research to enhance the accuracy of high-quantile predictions.

6.3 Extension to other models

Since it is known that the MA method generally performs well when the error variance is large (Liu et al. 2016, 2023), the proposed MA approach may apply to certain ‘sub-asymptotic’ extreme value distributions that suffer from high error variance in high quantile estimation. One example is the four-parameter kappa distribution (Hosking 1994; Shin & Park 2024; Strong et al. 2025), a generalization of the GEVD with one more shape parameter. Given that the MLE for the four-parameter kappa distribution exhibits high error variance (Papukdee et al. 2022), the MA method may provide a more reliable estimator than the MLE.

Extending the proposed method to non-stationary (NS) extreme value models would also be beneficial. In NS extreme value modeling, the MLE is highly sensitive to outliers or a few influential observations toward the end of the sample, often leading to substantial estimation variance for high quantiles. To address this issue, some researchers (Strupczewski & Kaczmarek 2001; Gado & Nguyen 2016) have proposed combining least squares and L-moment estimation methods. To fit an NS GEV model using the proposed MA approach, we first select K submodels with fixed shape parameters. In NS GEV modeling, the shape parameter (ξ_t) is difficult to estimate precisely, so we treat ξ as a constant. Under each fixed shape parameter ξ_k , we estimate the MLE of NS location and scale parameters. Next, the NS GEV submodel is transformed into a stationary extreme value model (Coles 2001). Under this transformed stationary model, the generalized L-moments distance is computed to assign weight to each submodel M_k . Further research is needed to explore this topic in greater detail.

7 Conclusion

We proposed a new MA method for estimating high quantiles of the GEVD. The proposed approach consists of selecting submodels based on the confidence interval of the shape parameter, estimating submodel parameters, and assigning weights to each submodel. Different criteria were employed for parameter estimation and weight assignment. Submodels were constructed using the MLE and LME, while weights were calculated using generalized L-moment distances and likelihood-based methods. This mixed approach, which leverages the strengths of both MLE and LME, is a key factor in improving accuracy when estimating high quantiles. Additionally, we quantified the uncertainty of the MA estimator for return levels under a random-weight setting. Furthermore, for further analysis, a surrogate model for the MA method was developed and applied to a real dataset—annual maximum daily precipitation in Hae-nam, Korea.

Based on our simulation study, the proposed MA method with the ‘gLd’ weighting scheme performed well for $-0.25 < \xi \leq 0$, while the MA method with the ‘like’ weighting scheme was effective for $\xi \leq -0.25$. In general, without considering specific values of ξ (i.e., tail heaviness), we recommend using the LME, the MA method with the ‘like’ weighting scheme, and the restricted MLE (or mixed estimator) considered by Morrison & Smith (2002) and Ailliot et al. (2011).

Funding and Acknowledgments

We thank Prof. Sanghoo Yoon for his help for this study. This research was supported by Basic Science Research Program through the National Research Foundation of Korea(NRF) funded by the Ministry of Education(RS-2023-00248434), and by Global - Learning & Academic research institution for Master’s, PhD students, and Postdocs(LAMP) Program of National Research Foundation of Korea(NRF) grant funded by Ministry of Education(No. RS-2024-00442775)

Code and data availability

Maximum rainfall data at Hae-nam, Korea: <https://github.com/yire-shin/MA-gev/tree/main/data>
R code for model averaging: <https://github.com/yire-shin/MA-gev.git>

Conflict of interest

The authors declare no potential conflicts of interest.

ORCID

Yire Shin, 0000-0003-1297-5430; Yonggwan Shin, 0000-0001-6966-6511
Jeong-Soo Park, 0000-0002-8460-4869

Author contributions statement

Park conceived the study, Yonggwan Shin and Yire Shin conducted the analysis. All authors wrote the first draft, reviewed, edited, and approved the final manuscript.

References

- [1] Ailliot, P., Thompson C., Thompson P. (2011). Mixed methods for fitting the GEV distribution. *Water Resour Res*, 47(5).
- [2] Allouche M, El Methni J, Girard S (2023). A refined Weissman estimator for extreme quantiles. *Extremes*, 26(3), 545-572.
- [3] Alvarez L, Chiann C, Morettin P (2022) Inference in parametric models with many L-moments. *arXiv:2210.04146*
- [4] Asquith WH (2014). Parameter estimation for the 4-parameter asymmetric exponential power distribution by the method of L-moments using R. *Comput Stat Data Anal*, 71, 955-970.
- [5] Bücher, A., Lilienthal, J., Kinsvater, P., Fried, R. (2021) Penalized quasi-maximum likelihood estimation for extreme value models with application to flood frequency analysis, *Extremes*, 24, 325–348.
- [6] Buckland, S. T., Burnham, K. P., Augustin, N. H. (1997). Model selection: An integral part of inference. *Biometrics*, 53, 603-618.
- [7] Casella G, Berger RL (2001). *Statistical inference*, 2nd ed., Duxbury.
- [8] Claeskens, G., Hjort, N. L. (2008). *Model selection and model averaging*. Cambridge: Cambridge Univ Press.

- [9] Coles, S. (2001). An introduction to statistical modeling of extreme values. London: Springer.
- [10] Coles SG, Dixon MJ (1999). Likelihood-Based Inference for Extreme Value Models. *Extremes*, 2, 5-23.
- [11] Daouia A, Padoan SA, Stupfler G (2024) Optimal weighted pooling for inference about the tail index and extreme quantiles. *Bernoulli* 30(2): 1287 - 1312.
- [12] Delicado P, Goría MN (2008) A small sample comparison of maximum likelihood, moments and L-moments methods for the asymmetric exponential power distribution. *Comput Stat Data Anal*, 52(3):1661-1673.
- [13] Elamir EA, Seheult AH (2004). Exact variance structure of sample L-moments. *J Stat Plann Infer*, 124(2), 337-359.
- [14] Evin G, Merleau J, Perreault L (2011) Two-component mixtures of normal, gamma, and Gumbel distributions for hydrological applications. *Water Resour Res* 47(8): W8525
- [15] Fabiola B, Cazzaniga G, De Michele C. (2021) Nonparametric extrapolation of extreme quantiles: A comparison study. *Stoch Envir Res Risk Assess* 36: 1579 - 1596.
- [16] Fletcher, D. (2018). Model Averaging. Berlin: Springer.
- [17] Gado TA, Nguyen VTN (2016) An at-site flood estimation method in the context of nonstationarity I. A simulation study. *J Hydro* 535:710-721.
- [18] Grego JM, Yates PA (2024). Robust Local Likelihood Estimation for Non-stationary Flood Frequency Analysis. *J Agri Bio Envir Stat*, 1-20. <https://doi.org/10.1007/s13253-024-00614-0>
- [19] Grego JM, Yates PA, Mai K (2015) Standard error estimation for mixed flood distributions with historic maxima. *Environmetrics* 26(3):229-242
- [20] Hansen BE, Racine J (2012) Jackknife model averaging, *J Econometrics*, 167:38-46.
- [21] Hao H, Huang B, Lee T-H (2024) Model averaging estimation of panel data models with many instruments and boosting. *J Appl Stat*, 51(1), 53-69.
- [22] Hjorth U (1982) Model selection and forward validation, *Scan J Stat* 9:95-105.
- [23] Hoeting, J., Madigan, D., Raftery, A., Volinsky, C. (1999). Bayesian model averaging: A tutorial. *Stat Sci*, 14(4), 382-417.
- [24] Hong J, Agustin W, Yoon S, Park J-S (2022) Changes of extreme precipitation in the Philippines, projected from the CMIP6 multi-model ensemble, *Weath Clim Extrem*, 37, 100480.
- [25] Hosking, J. R. M. (1990). L-Moments: Analysis and Estimation of Distributions Using Linear Combinations of Order Statistics. *J Royal Stat Soc B*, 52(1), 105-124.
- [26] Hosking, J.R.M.(1994): The four-parameter kappa distribution. *IBM Jour Res Devel*, 38(3):251-258.
- [27] Hosking, J. R. M., Wallis, J. R. (1997). *Regional Frequency Analysis: An Approach Based on L-moments*. UK: Cambridge University Press.
- [28] Katz RW, Parlange MB, Naveau P (2002) Statistics of extremes in hydrology, *Adv Water Resour* 25:1287-1304.
- [29] Karvanen, J. (2006). Estimation of quantile mixtures via L-moments and trimmed L-moments. *Comput Stat Data Anal*, 51(2), 947-959.
- [30] Kjeldsen TR, Ahn H, Prosdocimi I (2017) On the use of a four-parameter kappa distribution in regional frequency analysis. *Hydrol Sci J* 62:1354-1363.
- [31] Kjeldsen TR, Prosdocimi I (2015). A bivariate extension of the Hosking and Wallis goodness-of-fit measure for regional distributions. *Water Resour Res*, 51(2), 896-907.

- [32] Lekina A, Chebana F, Ouarda T.B.M.J. (2014) Weighted estimate of extreme quantile: An application to the estimation of high flood return periods. *Stoch Envir Res Risk Assess* 28: 147-165.
- [33] Liu, Q., Okui, R., Yoshimura, A. (2016). Generalized least squares model averaging. *Econometric Reviews*, 35(8-10), 1692-1752.
- [34] Liu, Z., Zheng, J., Tu, C., Pan, Y. (2023). Estimation for volunteer web survey samples using a model-averaging approach. *J Appl Stat*, 50(16), 3251-3271.
- [35] Lomba JS, Alves MIF (2020) L-moments for automatic threshold selection in extreme value analysis. *Stoch Envir Res Risk Assess* 34, 465-491
- [36] Morrison JE, Smith JA (2002). Stochastic modeling of flood peaks using the generalized extreme value distribution. *Water Resour Res*, 38(12).
- [37] Naghettini, M. (2017). *Fundamentals of Statistical Hydrology*. Springer.
- [38] Papukdee N, Park J-S, Busababodhin P (2022). Penalized likelihood approach for the four-parameter kappa distribution. *J Appl Stat*, 49(6), 1559-1573.
- [39] Raftery AE, Gneiting T, Balabdaoui F, Polakowski M (2005) Using Bayesian model averaging to calibrate forecast ensembles, *Month Weath Rev*, 133:1155-1174.
- [40] Ravishanker N, Chi Z, Dey DK (2022) *A First Course in Linear Model Theory*, 2nd ed., Chapman & Hall/CRC
- [41] Reiss R-D, Thomas M (2007) *Statistical analysis of extreme values*, 3rd ed. Birkhauser.
- [42] Sabourin A, Naveau P, Fougères AL (2013) Bayesian model averaging for multivariate extremes. *Extremes* 16, 325-350.
- [43] Salaki DT, Kurnia A, Sartono B, Mangku IW, Gusnanto A (2024). Model averaging in calibration of near-infrared instruments with correlated high-dimensional data. *J Appl Stat*, 51:279-297.
- [44] Serfling R J (1980) *Approximation theorems of mathematical statistics*, John Wiley & Sons.
- [45] Shin Y, Lee Y, Choi J, Park J-S (2019) Integration of max-stable processes and Bayesian model averaging to predict extreme climatic events in multi-model ensembles. *Stoch Envir Res Risk Assess*, 33:47-57.
- [46] Shin Y, Park J-S (2023) Modeling climate extremes using the four-parameter kappa distribution for r -largest order statistics. *Weath Clim Extrem*, 39:100533. (Revision at arxiv.org/abs/2007.12031v3)
- [47] Strong R, Borgstroem O, Nathan R, Wasko C, O'Shea D (2025) Global Applicability of the Kappa Distribution for Rainfall Frequency Analysis. *Water Resour Res*, 039035. <https://doi.org/10.1029/2024WR039035>
- [48] Strupczewski WG, Kaczmarek Z (2001) Non-stationary approach to at-site flood frequency modelling. Part II. Weighted least squares estimation. *J Hydro*, 48(14):143-151.
- [49] Totaro V, Kuczera G, Iacobellis V (2024) Goodness-of-fit, identifiability and extrapolation: Can the two-component extreme value distribution be used in at-site flood frequency analysis? *J Hydro*, 640: 131590
- [50] Vettori S, Huser R, Segers J, Genton MG (2020), Bayesian model averaging over tree-based dependence structures for multivariate extremes, *J Comput Graph Stat* 29:174-190
- [51] Wang H, Zhang X, Zou G (2009) Frequentist model averaging estimation: A review. *J Syst Sci Complex* 22, 732-748.
- [52] Zhang X, Zhang X (2023) Optimal model averaging based on forward-validation, *J Econometrics*, 237(2C): 105295.